Environmental Science
Processes & Impacts

PAPER

Cite this: *Environ. Sci.: Processes Impacts*, 2016, **18**, 1220

Concentration dynamics of coarse and fine particulate matter at and around signalised traffic intersections†

Prashant Kumar*[ab] and Anju Goel[a]

The understanding of rapidly evolving concentrations of particulate matter (PMC) at signalised traffic intersections (TIs) is limited, but it is important for accurate exposure assessment. We performed "mobile" and "fixed-site" monitoring of size-resolved PMCs in the 0.25–34 μm range at TIs. On-road mobile measurements were made inside a car under five different ventilation settings on a 6 km long round route, passing through 10 different TIs. Fixed-site measurements were conducted at two types (3- and 4-way) of TIs. The aims were to assess the effects of different ventilation settings on in-vehicle PMCs and their comparison during delay conditions at the TIs with those experienced by pedestrians while crossing these TIs. We also estimated the zone of influence (ZoI) for PM_{10}, $PM_{2.5}$ and PM_1 under different driving conditions and fitted the probability distribution functions to fixed-site data to understand the concentration and exposure dynamics of coarse and fine particles around the studied (3- and 4-way) TIs. The fine particles ($PM_{2.5}$) showed a strong positive exponential correlation with the air exchange rates under different ventilation settings compared with coarse particles ($PM_{2.5-10}$) showing an opposite trend. This suggested that the ventilation system of the car was relatively more efficient in removing coarse particles from the incoming outside air. On-road median PM_{10}, $PM_{2.5}$ and PM_1 during delays at the TIs were ~40%, 16% and 17% higher, respectively, compared with free-flow conditions on the rest of the route. About 7% of the average commuting time spent during delay conditions over all the runs at the TIs corresponded to 10, 7 and 8% of the total respiratory deposition dose (RDD) for PM_{10}, $PM_{2.5}$ and PM_1, respectively. The maximum length of the ZoI for $PM_{2.5}$ and PM_1 was highest at the 4-way TI and the maximum length of the ZoI for PM_{10} was highest at the 3-way TI. The on-road average RDD rate of PM_{10} inside the cabin when windows were fully open was up to ~7-times that for pedestrians at the TIs.

Received 1st April 2016
Accepted 4th August 2016

DOI: 10.1039/c6em00215c

rsc.li/process-impacts

Environmental impact

Signalised traffic intersections (TIs) are pollution hotspots that contribute disproportionately higher to overall commuting exposure. Studies characterising the exposure to coarse and fine particulate matter (PM) at such hotspots are yet limited. This study provides a comprehensive assessment of in-cabin exposure to fine and coarse PM under five different ventilation settings and compares in-cabin exposure at TIs with pedestrian exposure. The findings of this work advance our understanding of the zone of high PM pollution around TIs and assist in making an informed choice on ventilation settings of cars to limit exposure at such pollution hotspots.

1. Introduction

The World Health Organisation (WHO) has placed outdoor air pollution among the top ten health risks faced by human beings, which causes seven million premature deaths every year.[1] Epidemiological studies have provided real-world evidence of associations between concentrations of airborne particulate matter (PM) and adverse health outcomes such as respiratory and cardiovascular diseases.[2] In the year 2013, about 61% and 87% of the urban population in the European Union (EU) was exposed to PM_{10} (≤10 μm) and $PM_{2.5}$ (≤2.5 μm) concentrations exceeding the daily limit imposed by the WHO for outdoor air pollution.[3] This study also linked $PM_{2.5}$ exposure to 403 000 premature deaths in 2012 in the EU.[3] Signalised traffic intersections (TIs) are known as pollution hotspots but studies focusing on understanding the concentration dynamics of coarse ($PM_{2.5-10}$) and fine ($PM_{2.5}$) particles at and around such TIs are yet limited and therefore taken as the focus of this study.

[a]*Department of Civil and Environmental Engineering, Faculty of Engineering and Physical Sciences, University of Surrey, Guildford GU2 7XH, UK. E-mail: P.Kumar@surrey.ac.uk; Prashant.Kumar@cantab.net; Fax: +44 (0)1483 682135; Tel: +44 (0) 1483 682762*

[b]*Environmental Flow (EnFlo) Research Centre, Faculty of Engineering and Physical Sciences, University of Surrey, Guildford GU2 7XH, UK*

† Electronic supplementary information (ESI) available. See DOI: 10.1039/c6em00215c

Travelling time has increased over the years in the UK and elsewhere,[4] indicating a growing need for accurate exposure assessment during daily commuting. For example, the UK population spent about an hour each day in vehicles during commuting in 2013; the average trip time during the year 2013 increased by 16% from 20.4 min in 1995/1997.[4] Our recent study[5] has shown that in some cases as low as 2% of the commuting time spent at TIs could contribute as high as 25% of the total commuting exposure to particle number concentrations (PNCs). A similar contribution of exposure during commuting can be expected for particle mass concentrations (PMCs) but is currently unavailable.

As summarised in Table 1, a number of commuting exposure assessment studies have become available in recent years but similar studies focusing at TIs are still limited. Furthermore, there is a certain longitudinal distance along the road legs from the centre of a TI that experiences increased levels of exhaust emissions due to interruptions in vehicle speed at the traffic signals. In our previous work,[6] we defined this affected longitudinal length of the road as the zone of influence (ZoI) of a TI. The pollutant concentration in this zone can be many times higher compared with the rest of the route. For instance, Kim *et al.*[7] observed that the ZoI of a 4-way TI for oxides of nitrogen (NO_x) extends from −200 to 200 m from the centre of the TI under stop-and-go driving conditions. They found that about 200 to 1000 ppb of additional NO_x was observed within the ZoI compared with the rest of the route length. Goel and Kumar[6] found the length of the ZoI to be −11 to 134 m from the centre of a 4-way TI during multiple-stopping driving conditions. Studies assessing the ZoI for PM are currently unavailable, and hence the ZoI is estimated in this work for PM_{10} ($\leq$10 μm), $PM_{2.5}$ ($\leq$2.5 μm) and PM_1 ($\leq$1 μm) under diverse driving conditions at TIs.

Some studies have focused on in-vehicle exposure (Table 1) and fixed-site measurements of PM (Table 2) but studies covering diverse ventilation settings are yet limited. In this work, we have compared pedestrian exposure with in-vehicle exposure under five different ventilation settings. Such comparisons are important for understanding human exposure at these pollution hotspots and identify the driving and ventilation conditions that are favourable to reduce the exposure of in-vehicle occupants and passers-by at TIs.

Fitting of the probability distribution function (pdf) to pollutant concentration data allows the assessment of frequency ranges of concentrations experienced by urban dwellers,[8] besides assisting in evaluation of policies and emission intervention measures.[9–11] A number of past studies have fitted the pdf to air pollution data and details about these studies can be seen elsewhere.[12,13] However, there are hardly any studies that have attempted to fit the pdf to different PM types at TIs, which is one of the aims of this study.

The distinctive features that aim to fill the existing research gaps of this work are as follows. Firstly, as opposed to previous studies[14–19] that have analysed the effect of ventilation settings and traffic conditions on in-cabin PMCs at individual commuting routes, this study has assessed the effect of ventilation settings and driving conditions on in-cabin PMCs at pollution hotspots such as TIs. Secondly, this is the first time

Table 1 Summary of studies on in-cabin PMCs under different ventilation settings

Study	Equivalent ventilation setting	Instrument	City	Vehicle	Environment types	Parameter	PMC (μg m^{-3})
Int Panis *et al.*[14]	Set_2	TSI Dustrack 8520	Brussels	Citroën Jumpy (2007)	Urban area	PM_{10}	21.15 ± 4.67[a]
					University town	PM_{10}	17.05 ± 6.72[a]
					Rural area	PM_{10}	16.45 ± 2.62[a]
Weichenthal *et al.*[15]	Set_2	TSI Dustrack 8520	Toronto Vancouver Montreal	Chevrolet garnd caravans, 2009–2012	City	$PM_{2.5}$	6.60 (4.68–15.9)[b]
						$PM_{2.5}$	6.01 (1.37–10.7)[b]
						$PM_{2.5}$	13.6 (4.28–33.3)[b]
Suarez *et al.*[16]	Set_2	Dust-Track II, 8532	Santiago	Toyota Yaris (model: 2006), Subaru Forester (2000), and Subary Legacy (2005)	City	$PM_{2.5}$	46.5 ± 20.5[a]
Geiss *et al.*[17]	Set_2	GRIMM 1.108	Ispra	18 private cars	Town	PM_{10}	48.6 (0.9–332.3)[b]
						$PM_{2.5}$	26.9 (0.9–94.4)[b]
						PM_1	22.6 (0.8–82.9)[b]
Gulliver and Briggs[18]	Set_5	OSIRIS	Northampton	Ford Fiesta (1995)	City	PM_{10}	43 ± 23[a]
						$PM_{2.5}$	16 ± 16[a]
						PM_1	7 ± 10[a]
Knibbs and Dear[19]	Set_2	TSI Dustrack 8520	Sydney	Mitsubishi Magna (1998)	City	$PM_{2.5}$	27.30

[a] Standard deviation. [b] Range.

Table 2 Summary of a relevant literature review on fixed-site measurements of PMCs at the TIs[a]

Study	Instrument	Season	Type of TI	Distance from the TI (m)	Height of measurement (m)	City (country)	PM_{10} ($\mu g\ m^{-3}$)	$PM_{2.5}$ ($\mu g\ m^{-3}$)	PM_1 ($\mu g\ m^{-3}$)
Kaur *et al.*[46]	HFPS	Spring	4-way	3	1.5	London (UK)	—	27.5	—
He *et al.*[44]	Fluke 983	—	—	3	0.3	Mong Kok (Hong Kong)	130	—	—
Strak *et al.*[47]	HI	—	—	9	—	Amsterdam (Netherlands)	48	27	—
Friend *et al.*[48]	TEOM	Summer		5–10	2–3	Brisbane (Australia)	30.7	—	—
This study	GRIMM (1.107)	Winter	3-way	3	1.5	Guildford (UK)	39 ± 24	24 ± 20	20 ± 20
This study	GRIMM (1.107)	Winter	4-way	3	1.5	Guildford (UK)	32 ± 20	19 ± 11	15 ± 10

[a] HFPS = high flow personal samplers; HI = Harvard impactors; TEOM = Tapered Element Oscillating Microbalance.

the ZoI of four different types of TIs under varying driving conditions (stop-and-go as well as multiple-stopping) is estimated for PM_{10}, $PM_{2.5}$ and PM_1. Thirdly, a comparison of human exposure at (*i.e.* in-vehicle) and around (*i.e.* pedestrian) the TIs is presented to understand the dynamics of exposure at these hotspots. Finally, this is the first time the pdf is fitted to PM_{10}, $PM_{2.5}$ and PM_1 data at TIs. Such a fitting is important in assessing the frequency and variability in PMC exposure at TIs.

In summary, this work addresses various poorly understood questions: (i) what is the effect of different ventilation settings on in-vehicle PMCs on the overall route?, (ii) how do the concentration and exposure levels vary during congested traffic conditions at TIs compared with free-flow traffic conditions on the rest of the route?, (iii) how does the length of the zone of influence (ZoI) vary at different types of TIs under stop-and-go driving conditions?, (iv) what is the distribution of different PM types (PM_{10}, $PM_{2.5}$ and PM_1), and (v) how does exposure to different PM types differ at (*i.e.* on-road or inside the vehicle) and around (*i.e.* pedestrian) TIs?

2. Materials and methods

2.1 Site description

As a part of a comprehensive experimental programme,[5,6,12] we carried out "mobile" and "fixed-site" monitoring of size-resolved PMC in the 0.25–34 μm range in Guildford, Surrey. Guildford is a typical UK town that has 137 580 inhabitants.[20] Most of its traffic fleet, involving buses and trucks, run on diesel fuel. Around 32% of the passenger cars run on diesel while all the new cars coming on-road from 1 September 2015 comply with Euro 6 standards. The roads in the town usually experience congestion due to traffic during morning and evening peak hours. The car ownership in Guildford Borough is greater than the national level, with each household, on average, possessing about 1.5 cars compared with 1.16 cars nationally.[21]

The mobile measurements were performed inside a car on a 6 km long round route that passed through 10 different TIs (Fig. 1a). As described in our previous work,[6] based on the number of roads intersecting at these TIs and built-up area around a TI, these TIs were divided into four categories: (i) 4-way TI with no built-up area ($TI_{4w\text{-}nb}$), (ii) 4-way TI with a built-up area ($TI_{4w\text{-}wb}$), (iii) 3-way TI with no built-up area ($TI_{3w\text{-}nb}$), and (iv) 3-way TI with a built-up area ($TI_{3w\text{-}wb}$). Here, TIs with a built-up area were assumed to be those TIs that were located in a street canyon with continuous rows of buildings on both sides with an aspect ratio of 0.8 to 0.9. TIs with no built-up area were the TIs that were surrounded by residential or commercial buildings but these buildings with height from 6 to 12 m were placed far apart. Out of ten TIs, four (TI_1, TI_2, TI_4 and TI_6) were $TI_{4w\text{-}nb}$, three (TI_3, TI_7 and TI_9) were $TI_{3w\text{-}nb}$, one (TI_{10}) was $TI_{4w\text{-}wb}$ and the rest were $TI_{3w\text{-}wb}$. The average daily traffic flow on different roads intersecting at these TIs was obtained from the DoT.[22] The total traffic volume at a TI was estimated by summing the traffic flow on each of the roads intersecting at a TI. TI_8 and TI_7 cater to the highest traffic flow of 160 824 veh per day while it was lowest (9846 veh per day) at TI_3. Further description of the routes and the TIs can be seen elsewhere.[5,6]

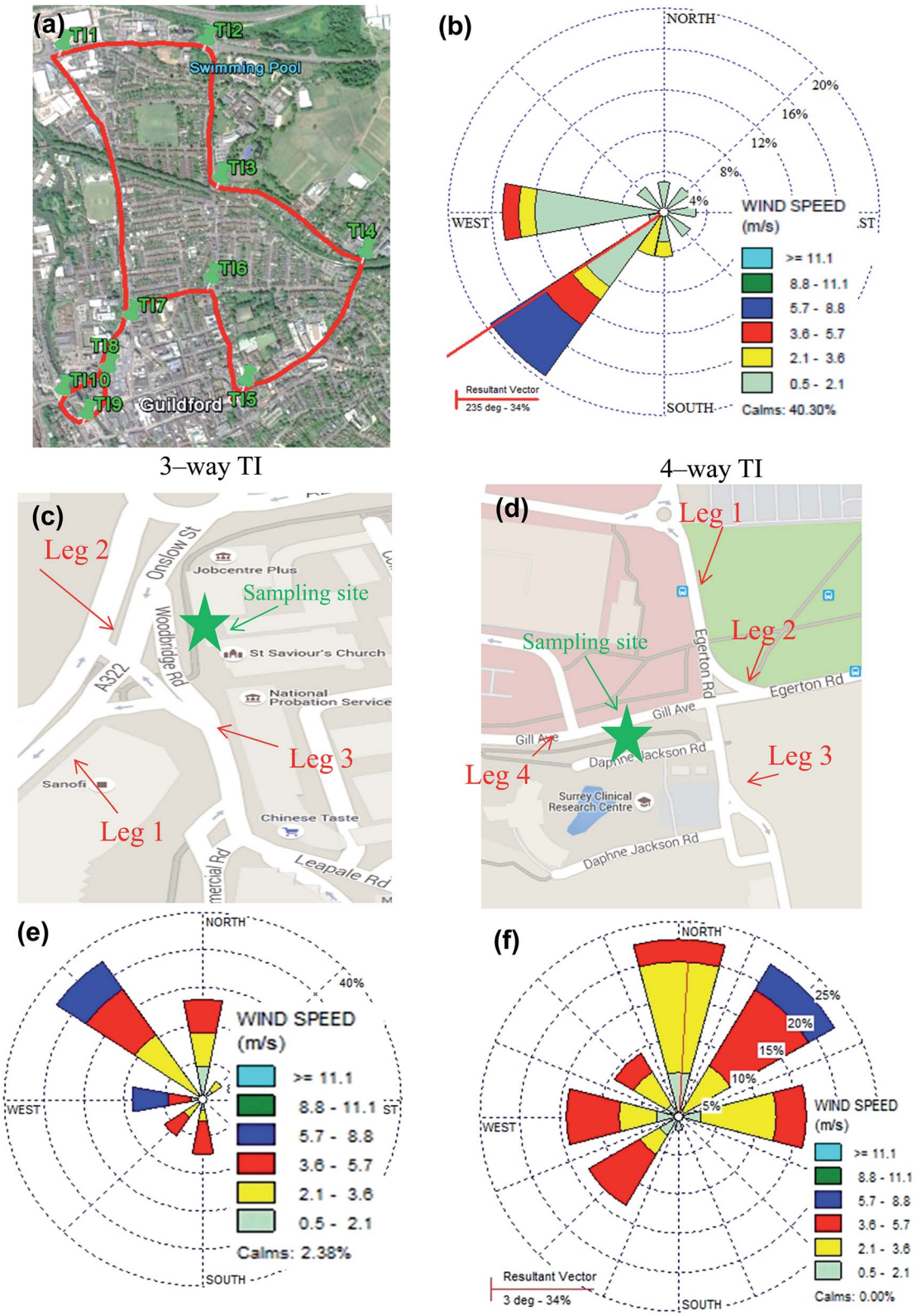

Fig. 1 (a) Map showing the location of ten TIs on the studied route for mobile measurements and the (b) wind rose diagram for the mobile monitoring period. Detailed google map showing the fixed site sampling location at (c) 3-way and (d) 4-way TIs. The wind rose diagram during the periods of fixed site monitoring at (e) 3-way and (f) 4-way TIs.

Fixed-site measurements were conducted at two different types (4- and 3-way) of TIs. The three-way TI is located in the city centre of Guildford and has three intersecting roads (legs 1, 2 and 3; Fig. 1c). The sampling location was around 4 m away from leg 2 in front of St. Savior's church. This TI has a signal cycle (*i.e.* total time of red, yellow and green lights) of around 83 s with the length of red light varying from 31 to 68 s on different legs of the TI. The four-way TI is located in a suburban area of Guildford and has 4 intersecting roads (*i.e.* legs 1, 2, 3 and 4; Fig. 1d). The sampling location was around 3 m away from leg 4 (Fig. 1d). This TI has a signal cycle of around 116 s; the length of the red light varied from 51 to 82 s on different legs of the TI. Further details on both these TIs can be seen in the study by Goel and Kumar.[12] The average daily traffic flow on different roads intersecting at both of these TIs was obtained from 5 minute manual traffic count every hour. The total traffic volume at a TI was estimated by summing the traffic flow on each of the roads intersecting at the TI (ESI Table S1†).

2.2 Instrumentation

Mobile measurements were conducted in a diesel-fuelled car (Ford Fiesta; 2002 registration; 1400 cc). The experimental car was equipped with a front disc brake and a rear drum brake system. The ventilation system was equipped with a roughly 8 month old pleated paper filter. There were three non-smoking occupants in the car, including the driver, during the measurements. The experimental car was equipped with filter-fitted ventilation and heating systems. A GRIMM spectrometer (model 1.107E) was deployed on the back seat of the car to measure PMD in the 0.25-34 μm size range at a sampling rate of 6 s. The instrument uses the optical scattering technique to classify the particles in 32 size channels. To ensure the quality of the collected data, first the instrument was calibrated in a three-step process by the manufacturer prior to on-site measurements. Secondly, we carried out on-site calibration by weighing (μg) the polytetrafluoroethylene (PTFE) filters that collected particle mass during the on-site measurements and compared these masses with the data of PM mass produced by the instrument.[23] The results of this comparison showed about 6% difference between the PMC estimated based on mass collected on a filter and the PMC given by the instrument and were therefore considered reliable. This instrument was successfully deployed in our previous studies during mobile[23] and indoor measurements,[24,25] where further details of its working principle, detection efficiencies and quality control of the data can be found. The position and speed of the vehicle were continuously recorded every second using a Global Positioning System (GPS; Garmin Oregon 350). A Panasonic HC-V500 camera was positioned on the dashboard of the car to take traffic videos at the time of measurements. Timestamps of all the instruments were matched in the beginning of the experiment to maintain the same starting time for collected data.

The same instrumentation set-up and sampling rate were used to collect the PMD data during the fixed-site measurements at both the TIs. Traffic flow videos at the TIs were continuously recorded for the entire monitoring period using the Panasonic HC-V500 camera. As in the case of mobile measurements, timestamps of all the instruments were matched in the beginning of each experiment.

2.3 Data collection

2.3.1 Mobile measurements. Measurements were conducted during morning and evening peak hours of March to April 2014. Travel was made in the north (N)–south (S) direction during morning peak hours and in the S–N direction during the evening hours with the intention of following the most agglomerated lanes. As described in Table 3,[5] the five different ventilation settings were used in order to assess their effect on in-cabin PMCs. Out of the total 74 runs, 43 runs were made during morning hours and the rest during the evening hours. The run time during morning and evening hours was almost similar (*i.e.* 16 ± 4 and 17 ± 4 min during morning and evening hours, respectively).

The air exchange rate (AER) of the experimental car was estimated for different settings (Table 3), using the methodology described in the study by Goel and Kumar.[5] The method uses

Table 3 Detailed descriptions of ventilation settings along with air exchange rate, AER[5] and number of runs during morning and evening peak hours in mobile monitoring

Setting	Description	AER ($m^3\ h^{-1}$)	No of runs in the morning	No of runs in the evening
Setting 1 (Set_1)	Windows fully open, fan and heating off. These measurements were considered equivalent to on-road measurements	—	12	10
Setting 2 (Set_2)	Windows closed, fan 25% and heating 50% on	125	5	6
Setting 3 (Set_3)	Windows closed, fan 100% on and heating off	257	7	6
Setting 4 (Set_4)	Windows closed, fan off and heating 100% on	16	5	9
Setting 5 (Set_5)	Windows closed, fan and heating off	17	14	—

decay rates of measured concentrations of carbon dioxide as a tracer gas. Each of the five ventilation settings was tested at least for 4 hours, except Set_1, for which 8 hours of measurements were collected. The meteorological data during the measurements were collected from a weather station located at Heathrow airport.[26] The meteorological data of this station have also been used by other studies carried out in Guildford.[5] During the measurement period, temperature and relative humidity inside the cabin were found to be 16 ± 3 °C and 51 ± 10%, respectively. The wind rose diagrams for the periods of sampling are shown in Fig. 1b. These diagrams classified the wind direction into 8 different categories: northwest (NW; 292.5–337.5°), north (N; 337.5–22.5°), northeast (NE; 22.5–67.5°), east (E; 67.5–112.5°), southeast (SE; 112.5–157.5°), south (S; 157.5–202.5°), southwest (SW; 202.5–247.5°) and west (W; 247.5–292.5°). By using the average wind speed and considering moderate incoming solar radiation during the measurements, atmospheric conditions were categorised as Pasquill stability class B during the measurements.[27]

2.3.2 Fixed-site measurements. Two different sets of measurements were conducted at the studied 3- and 4-way TIs. As described in Table 4, each of the two sets of measurements included monitoring at: (i) the corners of the TIs (*i.e.* ~1.5 m above the road level close to the breathing zone; these measurements are referred to as "fixed-site" measurements), (ii) at five different points (*i.e.* at 10, 20, 30, 45 and 60 m) away from the centre of TIs for the assessment of "horizontal decay profiles". A total of 75 600 data points of size-resolved PMDs were collected at a frequency of 6 s during a total of 126 h of fixed-site measurements at both the TIs. A total of 10 800 data points of size-resolved PMDs were obtained during 18 h of measurements for horizontal profiles at a sampling frequency of 6 s at both the legs of the 4-way TI. To acquire a representative data set at each sampling point, the samples were taken for 11 min in an hour at each sampling point, by manually repositioning the location of the instrument.

Fig. 1e and f show the wind rose diagram for the measurements at both the TIs. The hourly meteorological data (*i.e.* wind speed, wind direction, temperature and relative humidity) during all the measurements were obtained from the nearest meteorological station (*i.e.* the Royal Horticulture Society's garden in Wisley). The average wind speed, ambient temperature and relative humidity during the measurements were 3.0 ± 1.3 m s^{-1}, 9.0 ± 4.8 °C and 52.6 ± 14.6% at the 4-way TI, respectively. The corresponding values at the 3-way TI were 3.5 ± 1.9 m s^{-1}, 5.3 ± 2.7 °C and 63.5 ± 7.9%, respectively. The atmospheric condition is classified as Pasquill stability class B at both the TIs.

2.4 Estimation of local background PMCs

The background concentration changes from location to location depending on the sources and dispersion conditions, as shown by the various background concentration maps by DEFRA.[28] Following the approach used in our previous work,[6] we estimated local background PMCs for each run during the mobile measurements by taking the 5th percentile value of 30 s rolling average of the 6 s concentration time series.[29] This methodology was adopted to smooth the data and to exclude the impact of micro-scale variations on traffic emitted PM. The estimated values of background PM_{10}, $PM_{2.5}$ and PM_1 under each of the five ventilation settings are provided in ESI Table S2.†

For fixed-site measurements, local background PMCs were derived by using two different approaches. For the 4-way TI, we first monitored PMCs at an upwind background location. Given the identical meteorological conditions during the background and on-site measurements, the background measurements were assumed to be representative of the background PMCs for the 4-way TI on 28 April 2015. Comparison of our measured background and the estimated background using the on-site data indicated that the total background PMCs were equal to the 5th percentile of 6 s average PMC measured at the 4-way TI. Following this observation and the approach, the background PMCs were estimated for the rest of the days at the 4-way TI as well as at the 3-way TI. A similar approach has been used by previous studies to deduce local background levels.[6,29] Average background PM_{10}, $PM_{2.5}$ and PM_1 concentrations were found to be 22 ± 21, 16 ± 15 and 13 ± 15 μg m^{-3} at the 3-way TI, respectively. The corresponding values at the 4-way TI were 16 ± 10, 11 ± 6 and 8 ± 6 μg m^{-3}, respectively. Our estimated background values compare well with the urban background studies elsewhere. For example, the estimates of DEFRA[30] suggest urban background $PM_{2.5}$ concentration in the southern UK to be about 17 μg m^{-3} during the winter season.

2.5 Estimation of delay periods, ZoI, RDD rate and fitting of pdf at TIs

Delay at a TI is the time lost by commuters due to signal and traffic conditions.[5] There are different types of delays at TIs, serving different purposes. Control delay is a sum of three types of delays (acceleration, stop and deceleration); this is usually measured to analyse the effect of control such as traffic signal.[31] Following the approach used in our previous work,[5] velocity–time plots were drawn for identifying the locations where deceleration and acceleration occurred in the vicinity of a TI (ESI Fig. S1b†). Further, distance–time plots were made for

Table 4 Detailed descriptions of fixed-site monitoring at 3- and 4-way TIs

	Days and duration	
Type of measurements	3-way	4-way
Fixed-site	January and February (from 8:00 to 18:00 h)	February and April 2015 (from 8:00 to 20:00 h)
Horizontal	—	April 2015 (from 8:00 to 20:00 h)

calculating the corresponding delays (ESI Fig. S1a†). A delay event occurs at a TI under two types of driving conditions (*i.e.* stop-and-go and multiple stopping). There are always delay conditions at one leg of the TI (where the signal light is red) and simultaneously free-flow conditions on another leg (where the signal light is green). Due to simultaneous occurrence of different driving conditions at different legs of the TIs, it was not possible to segregate the data for delay events from the fixed-site measurements and, therefore, the waiting time at a TI when the signal is red is referred to as delay conditions hereafter in the text.

The ZoI represents the length of a road around a TI that is affected by higher particle mass emissions as compared to the rest of the route where free-flow driving conditions persist. The ZoI is estimated based on the intersecting points of driving speed *versus* distance, and PMCs *versus* distance, profiles at a TI. The example demonstrating the method to estimate the ZoI is shown in ESI Fig. S2.† For estimating the ZoI, PMC data for ±200 m distance from the centre of each of the TIs were extracted. This preliminary distance was chosen based on our prior field experience.[6] We observed that the effects of traffic lights on emissions die back to normal during free-flow traffic conditions by the end of about 200 m in each direction on the chosen route.[6] The ZoI was then estimated for delay conditions at the TIs.

The RDD rate for PM_{10}, $PM_{2.5}$ and PM_1 is estimated by using eqn (1):

$$\text{Deposited doses (in thoracic, tracheobronchial, alveolar regions) of PM fractions} = (V_T \times f) \times DF_i \times PM_i \quad (1)$$

where V_T is the tidal volume, f is the frequency of breathing, DF_i and PM_i are the deposition fraction and PMC of particle size i in μm. We used V_T as 800 cm^3 per breath and f as 0.35 for men during light exercise conditions.[32] DF_i is estimated for the mass median diameter (d_p) of PM_{10}, $PM_{2.5}$ and PM_1 based on eqn (2), given by Hinds.[32]

$$DF = IF\times \left(0.058 + \frac{0.911}{1+\exp(4.77+\ln d_p)} + \frac{0.943}{1+\exp(0.508-2.58\ln d_p)}\right) \quad (2)$$

where IF is the inhalable fraction that is computed as:

$$IF = 1 - 0.5\left(1 - \frac{1}{1+0.00076{d_p}^{2.8}}\right) \quad (3)$$

ESI Fig. S3† shows the method to estimate the mass median diameters for different PM fractions. The average DF for different ventilation settings in mobile measurements and at two types of TIs during fixed-site measurements is presented in ESI Table S3.†

At both the TIs, the statistical pdf was fitted to a total of 18 combinations, *i.e.* two monitoring locations × three different times (6 s, 15 min and 1 h) averages × three PM types (PM_{10}, $PM_{2.5}$ and PM_1). A total of 61 different statistical pdfs were tested on each of the 18 combinations and goodness of fit parameters were estimated by using the Anderson–Darling (A–D) method.[13] Based on a thorough visual inspection of the pdf plots and histograms and the goodness-of-fit test criteria, all the 61 distributions were ranked and the "best fit" distribution was selected for each of the 18 combinations. In order to identify the type of distribution that could fit the majority of the time averaged series of PMCs, a "common" distribution among the top ten ranked distributions was chosen.

3. Results and discussion

The size of particles is an important parameter to determine their sources and behaviour in the respiratory system. Therefore, measured PMCs have been divided into three sizes (PM_{10}, $PM_{2.5}$ and PM_1) for discussion. The overall framework of the results presented in this section is presented in ESI Fig. S4.†

3.1 On-road PMCs

As discussed in Section 2.3, on-road PMCs were measured inside the cabin with windows fully open (*i.e.* Set_1). Since contribution to coarse ($PM_{2.5-10}$) and fine ($PM_{2.5}$) particles comes from different sources, we discussed the obtained PMCs in these two different fractions (Fig. 2a). Coarse particles are usually dominated by the non-exhaust sources such as road abrasion, brake and tyre wear while fine particles are mainly due to fuel combustion in engines.[33] The on-road concentration of coarse particles during the evening runs (33 ± 9 μg m^{-3}) was found to be about twice that during morning runs (16 ± 4 μg m^{-3}); no such differences were observed for fine particles (Fig. 2a). This can be explained due to higher fugitive dust emissions during the evening.[34] These higher fugitive dust emissions can be expected during the evening hours compared with those during the morning hours due to a higher surface temperature of the road and a lower surface moisture content. The fraction of coarse particles, after subtracting the background, during the morning (69 ± 6%) and evening (77 ± 5%) hours dominated the total PMCs. These observations suggest that on-road coarse particles are principally affected by non-exhaust emissions during different hours in a day.

For comparison with the literature, we have estimated average on-road PM_{10}, $PM_{2.5}$ and PM_1 concentrations that were found to be 44, 21 and 14 μg m^{-3}, respectively (ESI Table S4†). A study by Chan *et al.*[35] was located for comparison where they measured PM_{10} (140 μg m^{-3}) and $PM_{2.5}$ (106 μg m^{-3}) concentrations inside a car in Guangzhou (China) with the windows fully open, using a TSI Dustrak 8520 model. The average PM_{10} and $PM_{2.5}$ concentrations reported by Chan *et al.*[35] were about 3- and 5-times higher than those observed in our study, respectively. Previous studies have reported about 1.8-times higher concentrations of $PM_{2.5}$ by using the TSI instrument compared with the GRIMM, contributing to some of the observed differences.[36] The remaining differences can possibly be explained by 3.5- and 4.5-times higher background PM_{10} (97 ± 26 μg m^{-3}) and $PM_{2.5}$ (72 ± 190 μg m^{-3}) concentrations in

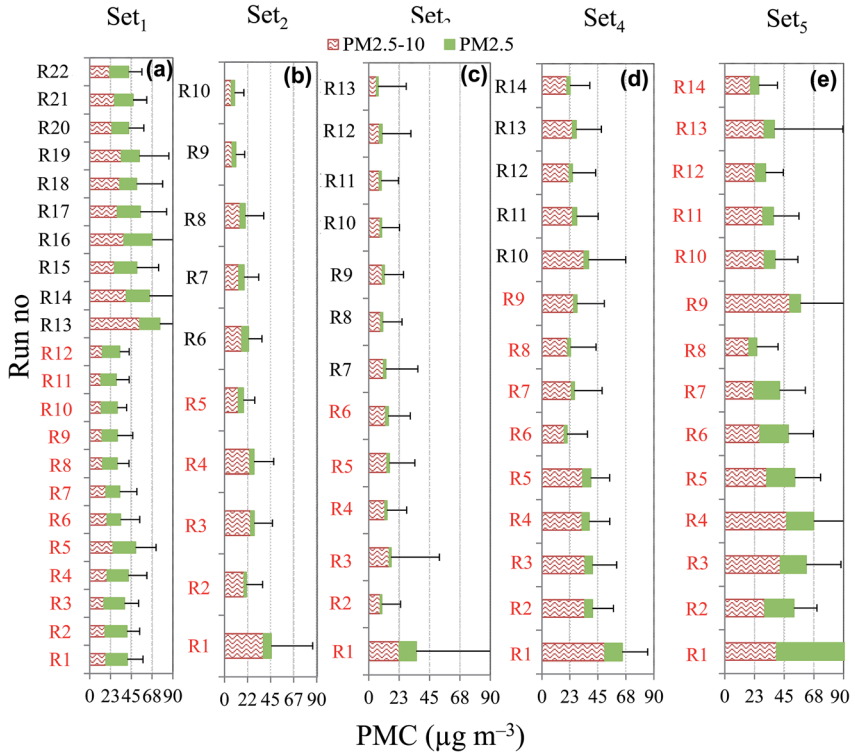

Fig. 2 In-cabin PMCs ($PM_{2.5-10}$ and $PM_{2.5}$) in two different fractions during (a) Set_1, (b) Set_2, (c) Set_3, (d) Set_4 and (e) Set_5. Please note that runs taken during morning hours are marked in red colour. For the sake of clarity only positive standard deviations are shown.

Chinese cities[37] compared with those estimated in our case (*i.e.* 28 ± 6 and 16 ± 2 μg m^{-3} of PM_{10}, and $PM_{2.5}$, respectively).

3.2 In-cabin PMC

Fig. 2b–d show the run-wise average of coarse and fine particles for in-cabin PMCs under four different ventilation settings (Set_2–Set_5). Contrary to Set_1, the concentration of coarse particles under Set_2 (which represents heating at 50% and fan at 25% on) during morning runs was found to be twice that during evening runs (12 ± 4 μg m^{-3}). No such variations were observed between the morning and evening runs for coarse or fine particles under the rest of the settings (Fig. 2b–d). The fraction of coarse particles constituted most of the PMCs under Set_2 (57%), Set_4 (76%) and Set_5 (69%), except Set_3 where fine particles dominated the PMC with the contribution of ~53% (ESI Table S4†). The higher fraction of fine particles under Set_3 could be due to higher AER since the infiltration of outside air with exhaust particles is expected to increase with the increase in AER.[38] This observation is substantiated by a strong positive exponential correlation ($R^2 = 0.95$) between AER and the fraction of fine particles for all settings as opposed to a negative exponential correlation ($R^2 = 0.95$) with coarse particles (ESI Fig. S5†). This positive correlation between AER and fine particles also suggests that the filters of the ventilation system are more efficient in removing coarse particles, compared with fine particles, from the incoming outside air.

The average in-cabin PM_{10} concentration was 31 ± 8, 23 ± 7, 38 ± 12 and 45 ± 14 μg m^{-3} under Set_2, Set_3, Set_4 and Set_5, respectively (ESI Table S4†). PM_{10} under Set_2 was within a factor of 2 of those reported by Int Panis *et al.*[14] for Brussels (Belgium) and Geiss *et al.*[17] for Ispra (Italy). This was presumably due to the effect of traffic volume (98 753 veh per day) in our study that was 1.9-times that reported by Int Panis *et al.*[14] with about 38% less vehicle speed than that in our case (21 km h^{-1}). No such data on traffic volume and driving speed were available for comparison with the work of Geiss *et al.*[17] Our PM_{10} under Set_5 (windows closed, fan and heating off; 45 ± 14 μg m^{-3}) compared well with that measured (43 ± 23 μg m^{-3}) by Gulliver and Briggs[18] in Northampton, UK (Table 1). This similarity can be expected given that both these studies were carried out in a typical UK town during the winter season and the route selected in both the studies was heavily trafficked with frequent queuing and congestion.

The average PM_{10} after subtracting the background was found to be highest under Set_5 and lowest under Set_3 (ESI Table S4†). The possible explanation for this could be different AERs under these settings. A strong negative linear correlation ($R^2 \approx 0.94$) between AER and PM_{10} under different ventilation settings suggests that there will be a decrease in dilution (and hence an increase in PM_{10}) with the decrease in AER. Interestingly, the relationship between AER and PM_{10} concentration is opposite to what is usually observed between AER and airborne nanoparticles[5] that is represented by PNCs.[39,40] This indicates that coarse particles and nanoparticles behave differently under different ventilation settings.

As for fine particles, average in-cabin $PM_{2.5}$ was found to be 13 ± 5, 12 ± 4, 9 ± 3 and 14 ± 7 μg m^{-3} under Set_2, Set_3, Set_4 and

Set_5, respectively (ESI Table S4†). The $PM_{2.5}$ concentration under Set_2 was within a factor of 2 of those reported by Weichenthal *et al.*[15] in Toronto (6.6 μg m^{-3}) and Montreal (13.6 μg m^{-3}), Canada, and Geiss *et al.*[17] in Ispra (13.6 μg m^{-3}), Italy. The $PM_{2.5}$ concentration under Set_5 (14 ± 7 μg m^{-3}) was identical to that measured (16 ± 16 μg m^{-3}) by Gulliver and Briggs[18] in Northampton, UK (Table 1). The average $PM_{2.5}$ after subtracting the background was highest under Set_2 and Set_3 and lowest under Set_4 (ESI Table S4†). The highest $PM_{2.5}$ under Set_2 and Set_3 can be explained by greater intake of outside air due to high AER under these settings as compared to Set_4.

Average in-cabin PM_1 was found to be 9 ± 4, 11 ± 4, 5 ± 2, and 9 ± 5 μg m^{-3} under Set_2, Set_3, Set_4 and Set_5, respectively (ESI Table S4†). Contrary to PM_{10}, a strong positive linear correlation (R^2 = 0.58) was observed between AER and average PM_1 under different ventilation settings. This indicates that penetration of exhaust particles inside the cabin decreases with a decrease in AER, resulting in decreasing in-cabin PM_1. Comparison of our results suggests that PM_1 for Set_2 is well within the range of those reported by Geiss *et al.*[17] (*i.e.* 0.8–82.9 μg m^{-3}) in Ispra (Italy). Likewise, PM_1 under Set_5 compares well with that measured by Gulliver and Briggs[18] (*i.e.* 7 ± 10 μg m^{-3}) in Northampton, UK (Table 1).

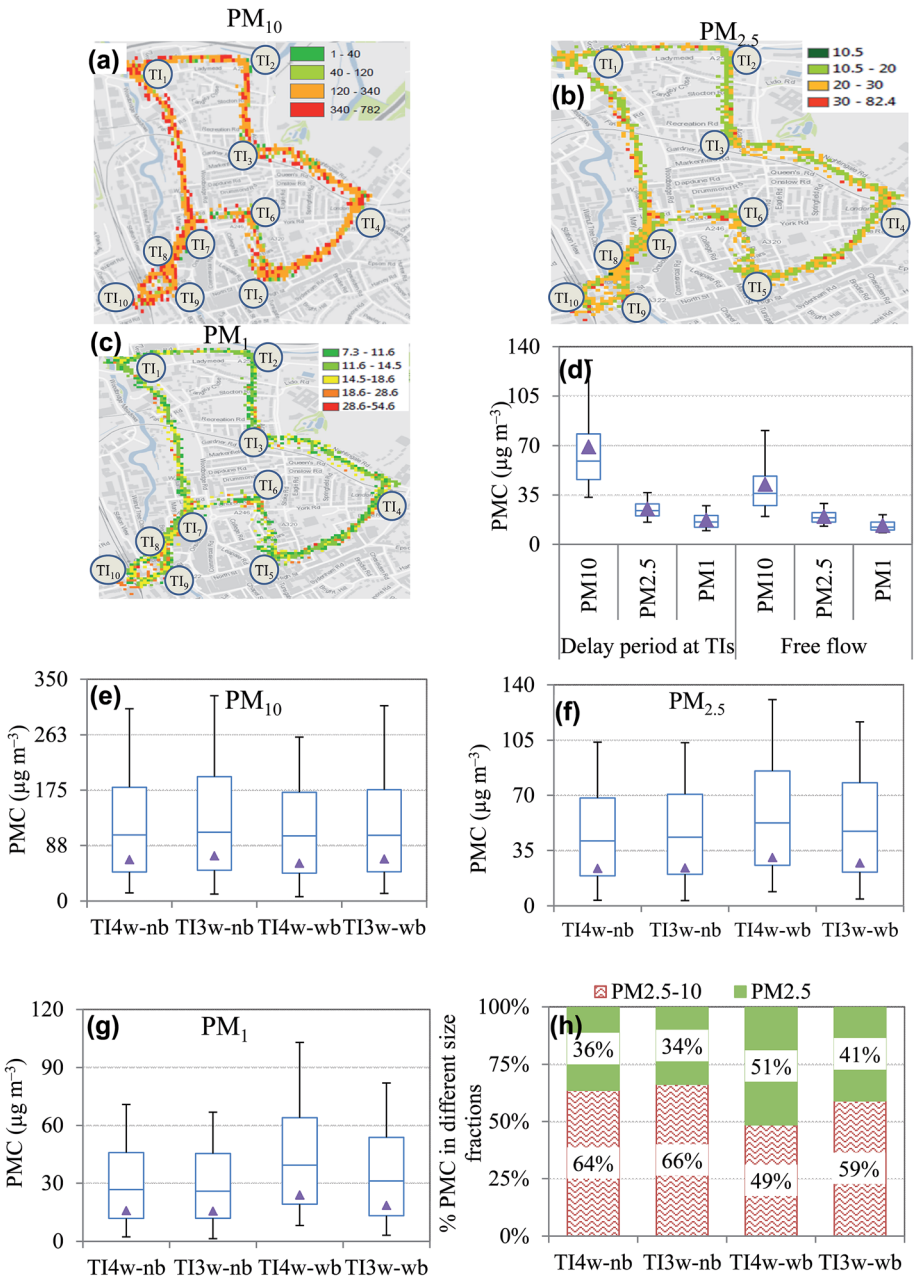

Fig. 3 Spatial variation of average (a) PM_{10}, (b) $PM_{2.5}$ and (c) PM_1 concentration during ventilation Set_1 on the whole route. (d) Average PM_{10}, $PM_{2.5}$ and PM_1 concentration during delays at all TIs and free-flow on the rest of the route. Average (e) PM_{10}, (f) $PM_{2.5}$ and (g) PM_1 concentration during delay conditions at four different types of TIs. (h) Percentage fraction of coarse ($PM_{2.5-10}$) and fine ($PM_{2.5}$) particles during delay conditions at four different types of TIs.

3.3 Spatial variations in PMCs

Fig. 3a–c show the spatially averaged plots of 6 s averaged PM_{10}, $PM_{2.5}$ and PM_1 concentrations on the studied route using the data collected for Set_1 (*i.e.* windows fully open, representing on-road PMCs). Consistently higher PM_{10} was observed near the TIs (Fig. 3a–c), mainly due to relatively higher non-exhaust emissions due to break and tyre wear[41] at the TIs compared with free-flow conditions. Likewise, relatively higher exhaust emissions are expected at the TIs, contributing to increased $PM_{2.5}$ and PM_1 levels, because of larger fuel consumption in congested traffic conditions compared with free flow traffic conditions on the rest of the route.[5]

To further assess the effect of congested conditions at TIs on PMCs, the concentrations of PM_{10}, $PM_{2.5}$ and PM_1 were segregated for delay and non-delay conditions at all the TIs on the studied route using the approach explained in Section 2.5 (Fig. 3d). Median PM_{10}, $PM_{2.5}$ and PM_1 during the delay period at the TIs were found to be 57, 23 and 15 $\mu g\ m^{-3}$, respectively; these were 40%, 16% and 17% higher than the corresponding values on the rest of the route with free-flow traffic conditions.

In addition to traffic driving conditions, geometries and the built-up area around TIs also affect the dispersion of PM emissions and hence the PMCs. To analyse the effect of geometries and the built-up area around the TI on PM fractions, we further divided our TIs into the following 4 categories based on the surrounding built-up area: $TI_{4w\text{-}nb}$, $TI_{3w\text{-}nb}$, $TI_{4w\text{-}wb}$ and $TI_{3w\text{-}wb}$. The results are summarised in Table 5 and the average PM is shown in Fig. 3e–h.

Median PM_{10} was found to be 59, 60, 59 and 58 $\mu g\ m^{-3}$, $PM_{2.5}$ as 22, 24, 27 and 26 $\mu g\ m^{-3}$ and PM_1 as 15, 14, 20 and 18 $\mu g\ m^{-3}$ at $TI_{4w\text{-}nb}$, $TI_{3w\text{-}nb}$, $TI_{4w\text{-}wb}$, and $TI_{3w\text{-}wb}$, respectively (Table 5). Interestingly, the median PM_{10} was almost approximately similar at all four categories of TIs (Table 5), indicating that the built-up environment has very little effect due to its relatively larger setting velocity. This was not the case for the median $PM_{2.5}$ and PM_1, which were highest at $TI_{4w\text{-}wb}$ where the traffic volume was also largest compared with other TIs with a built-up area (*i.e.* 93 340, 85 335, 108 554, 107 784 veh per day at $TI_{4w\text{-}nb}$, $TI_{3w\text{-}nb}$, $TI_{4w\text{-}wb}$ and $TI_{3w\text{-}wb}$, respectively). Moreover, accumulation of fine PMCs at the TIs with built-up area is expected to be higher due to limited dilution than the TIs with no built-up area.[42]

The above discussions show that delay conditions at TIs can result in 40%, 16% and 17% higher PM_{10}, $PM_{2.5}$ and PM_1, respectively, compared with those on the rest of the route with free-flow conditions. The effect of built-up area around a TI on PM_{10} was almost non-existent. Conversely, an increase of about 10% and 30% in median $PM_{2.5}$ and PM_1 was found at TIs with a built-up area compared with TIs with no built-up area.

3.4 ZoI at the TIs under different driving conditions

Delay conditions affect the certain length of the road around a TI, which is referred to as ZoI.[6] The longitudinal distance, representing the ZoI at the TIs, is estimated using the method explained in Section 2.5. The ZoI is expected to vary for different fractions of PM due to their distinct sources.[33] This section discusses the extent of the ZoI for three different fractions of PM (PM_{10}, $PM_{2.5}$ and PM_1) at four different categories of TIs ($TI_{4w\text{-}nb}$, $TI_{4w\text{-}wb}$, $TI_{3w\text{-}nb}$ and $TI_{3w\text{-}wb}$) for delay events during stop-and-go and multiple-stopping driving conditions, which occur frequently at the TIs. Each of the studied 10 TIs was divided into the above-mentioned four categories of TIs and then the ZoI at each of the 10 TIs during each individual run was derived (ESI Tables S5–S10†). These runs were then divided into stop-and-go and multiple stopping driving conditions. A summary of ZoI ranges (*i.e.* maximum, minimum, median and average) for stop-and-go and multiple stopping driving conditions is presented in Table 6 and ESI Table S11,† respectively.

Comparison of different ranges of ZoI suggests that the maximum length of the ZoI was found to be up to 1.5, 1.6 and 1.7-times the median length for PM_{10}, $PM_{2.5}$ and PM_1, respectively, under both driving conditions at all the TIs. The median length was within ±5% of the average length of the ZoI for all fractions of PM (Table 6 and ESI Table S11†). Given that the maximum and median values are most relevant for both the driving conditions; these are chosen for the subsequent discussions.

Table 5 Average and median PM_{10}, $PM_{2.5}$ and PM_1 concentrations at four different types of TIs

	PM_{10} ($\mu g\ m^{-3}$)		$PM_{2.5}$ ($\mu g\ m^{-3}$)		PM_1 ($\mu g\ m^{-3}$)	
Type of TI	Average ± σ	Median	Average ± σ	Median	Average ± σ	Median
TI_1	69 ± 36	61	23 ± 5	23	15 ± 4	16
TI_2	72 ± 32	65	19 ± 3	20	13 ± 2	12
TI_4	53 ± 20	45	27 ± 10	24	19 ± 6	19
TI_6	63 ± 15	58	28 ± 6	29	18 ± 6	21
$TI_{4w\text{-}nb}$	**65 ± 29**	**59**	**24 ± 7**	**22**	**16 ± 5**	**15**
TI_3	49 ± 4	49	21 ± 4	21	16 ± 3	18
TI_7	65 ± 31	58	23 ± 5	23	16 ± 5	13
TI_9	85 ± 35	86	26 ± 6	26	15 ± 4	14
$TI_{3w\text{-}nb}$	**71 ± 33**	**60**	**24 ± 5**	**24**	**16 ± 4**	**14**
TI_{10}	59 ± 19	59	31 ± 14	27	24 ± 14	20
$TI_{4w\text{-}wb}$	**59 ± 18**	**59**	**31 ± 14**	**27**	**24 ± 14**	**20**
TI_5	80 ± 34	75	24 ± 4	24	14 ± 3	14
TI_8	63 ± 36	56	28 ± 8	27	20 ± 8	20
$TI_{3w\text{-}wb}$	**66 ± 36**	**58**	**27 ± 8**	**26**	**19 ± 7**	**18**

Table 6 Maximum, minimum, median and the average length of the ZoI for PM_{10}, $PM_{2.5}$ and PM_1 at four different categories of TIs during stop-and-go driving conditions. X_1 and X_2 are starting and end points of the ZoI as described in Section 2.5. Please note that some of the X_2 values are positive since they represent instances when the TI was fully saturated and a vehicle had to stop much before the stop line due to congestion

	Max			Min			Median			Average		
Type of TIs	X_1 (m)	X_2 (m)	Length (m)	X_1 (m)	X_2 (m)	Length (m)	X_1 (m)	X_2 (m)	Length (m)	X_1 (m)	X_2 (m)	Length (m)
PM_{10}												
$TI_{4w\text{-}nb}$	189	49	140	0	−96	96	86	−26	112	89	−33	121
$TI_{3w\text{-}nb}$	200	14	186	11	−47	58	126	3	123	100	−16	116
$TI_{4w\text{-}wb}$	100	58	42	55	−20	75	69	29	40	75	20	55
$TI_{3w\text{-}wb}$	156	68	88	22	−100	122	86	−37	123	86	−32	118
$PM_{2.5}$												
$TI_{4w\text{-}nb}$	194	20	174	38	−16	54	110	−5	116	106	−9	114
$TI_{3w\text{-}nb}$	171	43	128	25	−47	72	90	9	81	92	2	90
$TI_{4w\text{-}wb}$	96	44	52	46	−23	69	79	11	68	76	11	65
$TI_{3w\text{-}wb}$	196	68	128	0	−100	100	85	−36	121	93	−32	125
PM_1												
$TI_{4w\text{-}nb}$	194	44	150	31	−16	47	114	13	102	107	−6	113
$TI_{3w\text{-}nb}$	164	19	145	20	−64	84	91	7	85	92	−13	105
$TI_{4w\text{-}wb}$	113	30	83	54	−23	77	86	5	81	76	11	65
$TI_{3w\text{-}wb}$	190	68	122	0	−100	100	60	−20	80	74	−25	99

There are some common features between both the driving conditions. For example, the maximum length of the ZoI for $PM_{2.5}$ and PM_1 was highest at $TI_{4w\text{-}nb}$ under both the driving conditions. Irrespective of the PM type, a negative linear correlation has been observed between the maximum length of the ZoI and average acceleration (*i.e.* $R^2 = 0.35$, 0.50 and 0.50 for PM_{10}, $PM_{2.5}$ and PM_1, respectively, under stop-and-go driving conditions; the corresponding values for multiple stopping are $R^2 = 0.59$, 0.86 and 0.98). These observations suggest that irrespective of the driving condition, the maximum length of the ZoI depends on acceleration.

Apart from some commonalities (discussed above), distinct features of the ZoI were also observed under both the driving conditions. For example, both maximum and median lengths of the ZoI were largest for PM_{10} at $TI_{3w\text{-}nb}$ under stop-and-go driving conditions. On the other hand, corresponding lengths for PM_{10} were highest at $TI_{3w\text{-}wb}$ under multiple stopping driving conditions. Similarly, the median length of the ZoI during stop-and-go driving conditions was highest for $PM_{2.5}$ and PM_1 at $TI_{3w\text{-}wb}$ and $TI_{4w\text{-}nb}$, respectively (Table 6) while the corresponding ZoIs for $PM_{2.5}$ and PM_1 were highest at $TI_{3w\text{-}nb}$ (ESI Table S11†) during multiple stopping conditions. Under stop-and-go driving conditions, a positive linear correlation was observed between the median length of the ZoI and the average driving speed for $PM_{2.5}$ ($R^2 = 0.35$) and PM_1 ($R^2 = 0.95$) while a negative linear correlation was observed between the median length of the ZoI and the average deceleration for $PM_{2.5}$ ($R^2 = 0.24$) and PM_1 ($R^2 = 0.68$) during multiple stopping driving conditions. No such correlation was seen for PM_{10} under both the driving conditions.

The above discussions clearly show that the ZoI exists within the vicinity of a TI and the length of a ZoI is dissimilar for different fractions of PM at different types of TIs. For stop-and-go driving conditions, the ZoI depends on the average acceleration and driving speed of traffic while it depends on the average acceleration and deceleration of traffic under multiple stopping driving conditions.

3.5 Fixed-site measurements at the 3- and 4-way TIs

The diurnal profiles of three different types of PM (*i.e.* PM_{10}, $PM_{2.5}$ and PM_1) at 3- and 4-way TIs are shown in Fig. 4a. At both the TIs, the diurnal profiles of $PM_{2.5}$ and PM_1 show the morning and evening peaks of traffic volume, indicating that both $PM_{2.5}$ and PM_1 are directly influenced by road traffic. The diurnal profile of PM_{10} also showed an additional afternoon peak that can be explained by fugitive dust emissions that are likely to be highest around mid-afternoon when the surface temperature was maximum, the surface moisture content was minimum, and the mean wind speed was highest due to thermally induced air movement.[43]

The percentage fraction of fine and coarse particles was almost similar at the 3- and 4-way TIs (Fig. 4b), indicating common exhaust and non-exhaust sources at both the TIs. The average PM_{10}, $PM_{2.5}$ and PM_1 at the 3-way TI were 39 ± 24, 24 ± 20 and 20 ± 20 μg m^{-3}, respectively, with the corresponding values at the 4-way TI being 32 ± 20, 19 ± 11 and 15 ± 10 μg m^{-3} (Table 7). On comparison, it was found that the PM_{10} at both 3- and 4-way TIs was within a factor of 2 of those reported in published literature (Table 2), except for the report by He *et al.*[44] who found over 3-times higher PM_{10} than those found at the studied 4-way TI. This can be explained by 3.5-times higher average background PM_{10} in the work of He *et al.*[44] compared with our background PM_{10} levels (ESI Table S2†). Similarly, the $PM_{2.5}$ reported at both the TIs was within ±20% of those reported in the literature (Table 2).

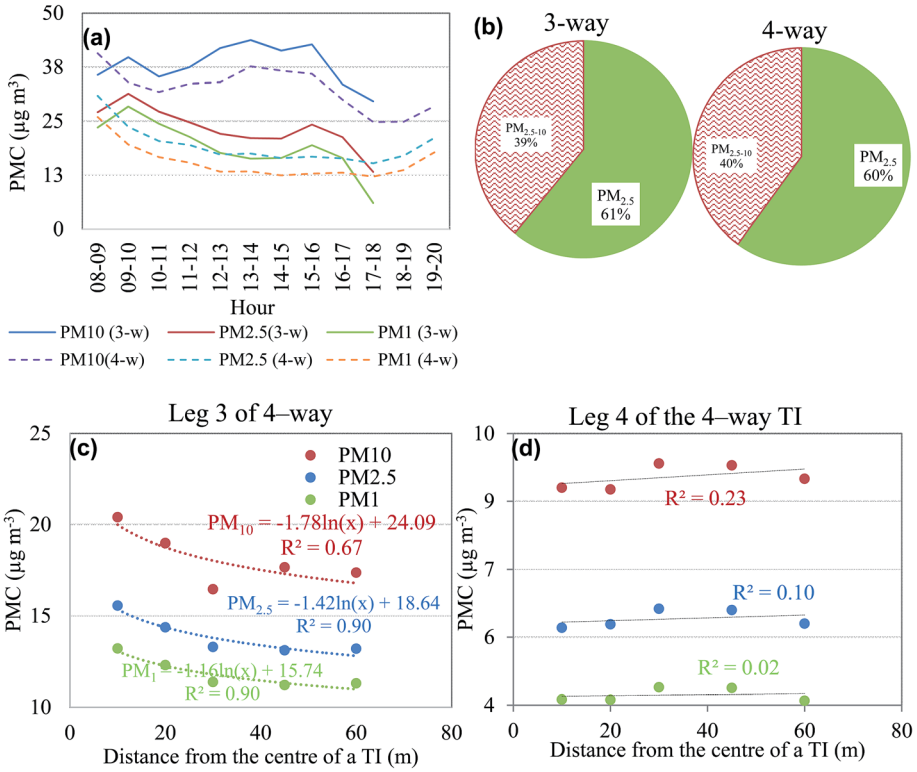

Fig. 4 (a) Diurnal profile of PM_{10}, $PM_{2.5}$ and PM_1 at 3- and 4-way TIs. (b) Percentage contribution of fine and coarse particles to PM_{10} concentrations at 3- and 4-way TIs. Horizontal profile of PM_{10}, $PM_{2.5}$ and PM_1 on (c) leg 3 and (d) leg 4 of a 4-way TI.

Table 7 Average, median and maximum PM_{10}, $PM_{2.5}$ and PM_1 concentration along with traffic volume and wind speed at 3- and 4-way TIs

Type of TI	Parameter	PM_{10} (μg m^{-3})	$PM_{2.5}$ (μg m^{-3})	PM_1 (μg m^{-3})	Traffic volume, veh per h (% diesel vehicle)	Wind speed (m s^{-1})
3-way	Average ± σ	39 ± 24	24 ± 20	20 ± 20	5498 ± 540 (43%)	3.5 ± 1.9
	Median	30	12	6	—	—
	Max	88	69	66	—	—
4-way	Average ± σ	32 ± 20	19 ± 11	15 ± 10	5014 ± 1172 (39%)	3.0 ± 1.3
	Median	29	16	12	—	—
	Max	108	56	52	—	—

3.6 Probability distribution fitting to PMCs during fixed-site measurements

Frequency histograms showing the range of PMCs and their corresponding likelihood (*i.e.* frequency of occurrence) are potentially more representative of exposure at TIs as compared to average or median PMCs.[11,45] Based on the frequency histograms, hourly averaged PM_{10} at the 3- and 4-way TIs for 99% of the total sampling duration was found to be ≤84 and 104 μg m^{-3}, respectively. The corresponding hourly averaged values for $PM_{2.5}$ were ≤62 and 51 μg m^{-3} and for PM_1 as ≤59 and 48 μg m^{-3}, respectively.

ESI Fig. S6† shows frequency histograms that are used to assess the frequency of violation of PM_{10}, $PM_{2.5}$ and PM_1 concentrations against the corresponding PMCs during free-flow (*i.e.* 41, 20 and 12 μg m^{-3} for PM_{10}, $PM_{2.5}$ and PM_1, respectively; Section 3.2). The hourly averaged PM_{10} at the 3- and 4-way TIs was found to exceed the average on-road (in-vehicle with windows fully open) free-flow PM_{10} concentration for 41% and 24% of the total time, respectively. The hourly averaged $PM_{2.5}$ exceeded the corresponding free-flow concentrations for 35% and 34% of the total time at the 3- and 4-way TIs, respectively. The hourly averaged PM_1 was found to exceed the average on-road PM_1 during free flow traffic conditions for 35% and 40% of the total time at the 3- and 4-way TIs, respectively.

The types of pdf vary for different time averages (Section 2.5). Therefore, distribution was fitted to 1 s, 15 min and 1 h averaged total PM_{10}, $PM_{2.5}$ and PM_1 concentrations at the 3- and 4-way TIs in order to assess the effect of time averages on the pdf fit. The summary of these outcomes is presented in Table 8, which shows the "best" and the "common" fit distributions of the PM_{10}, $PM_{2.5}$ and PM_1 for three different averaging periods.

Table 8 Best fit and common fit distributions for PM_{10}, $PM_{2.5}$ and PM_1 concentrations at 3- and 4-way TIs

Types of TIs	Type of fit	Averaging time	PM_{10}	$PM_{2.5}$	PM_1
3-way TI	Best fit	6 s	Inverse Gaussian	Burr	GEV
		15 min	Inverse Gaussian	Inverse Gaussian	Inverse Gaussian
		1 h	Gamma	Inverse Gaussian	Gamma
	Common fit		Inverse Gaussian	Inverse Gaussian	Inverse Gaussian
4-way TI	Best fit	6 s	GEV	Inverse Gaussian	Inverse Gaussian
		15 min	Exponential	Gamma	GEV
		1 h	Weibull	Gamma	Gamma
	Common fit		Gamma	Gamma	Gamma

Irrespective of PM type, inverse Gaussian is found to be the "common" fit at the 3-way TI while it is the Gamma distribution that is a "common" fit for the 4-way TI. Inverse Gaussian was found to be the best fit for 15 min averaged PM_{10}, $PM_{2.5}$ and PM_1 at the 3-way TI and 6 s averaged $PM_{2.5}$ and PM_1 data at the 4-way TI. The best fit distribution describes the pdf of specific time averaged PMC data well while common fit distribution is the type of distribution that could fit the majority of the time averaged series of PMCs adequately. This knowledge about statistical distributions that fit well to PMC data at different types of TIs can be important for assessing the frequency of violation of air quality standards and designing mitigation strategies.

3.7 Horizontal decay of PM along the road length at the TI

To analyse the horizontal variation in the PMCs, measurements were carried out at five different distances from the centre of the TI on two different legs (3 and 4) of the 4-way TI (Fig. 4c and d). All three types of PMCs (with $R^2 = 0.71$, 0.90 and 0.90 for PM_{10}, $PM_{2.5}$ and PM_1, respectively) were found to decay logarithmically with increasing distance from the centre of a TI at leg 3 while no such decays were observed at leg 4 of the studied TI (Fig. 4c and d). The decay profiles of PMCs are different from those observed for airborne nanoparticles at this TI where an exponential decay ($R^2 = 0.68$–0.71) was observed with increasing distance from the centre of the TI at both the legs of the studied TI.[12] The differences in decay profiles of different PM types and nanoparticles can be explained by their origin. For example, PM_{10} emissions mainly come from resuspension of dust and tyre wear (Section 3.3) while nanoparticles and PM_1 are from exhaust emissions.[48–50]

3.8 Exposure assessment

3.8.1 On-road and pedestrian exposure at the TIs. The RDD rate during Set_1 (*i.e.* windows fully open) is considered as a representative of on-road RDD rate and fixed-site measurements at the TIs as pedestrian exposure. The average on-road RDD rate of PM_{10} (80 μg h^{-1}), $PM_{2.5}$ (7 μg h^{-1}) and PM_1 (3 μg h^{-1}) during the delay period at TIs was found to be about 55%, 5% and 17% higher than those during the rest of the run periods (Fig. 5a–c). Short-term exposure to PM_{10} under delay conditions at TIs can contribute to a reasonable proportion of commuting exposure. For instance, the average percentage of time spent under delay conditions over all the runs at TIs was about 7% of the total commuting time, but this contributed to 10, 7 and 8% of the total RDD during this run for PM_{10}, $PM_{2.5}$ and PM_1, respectively (ESI Table S12†).

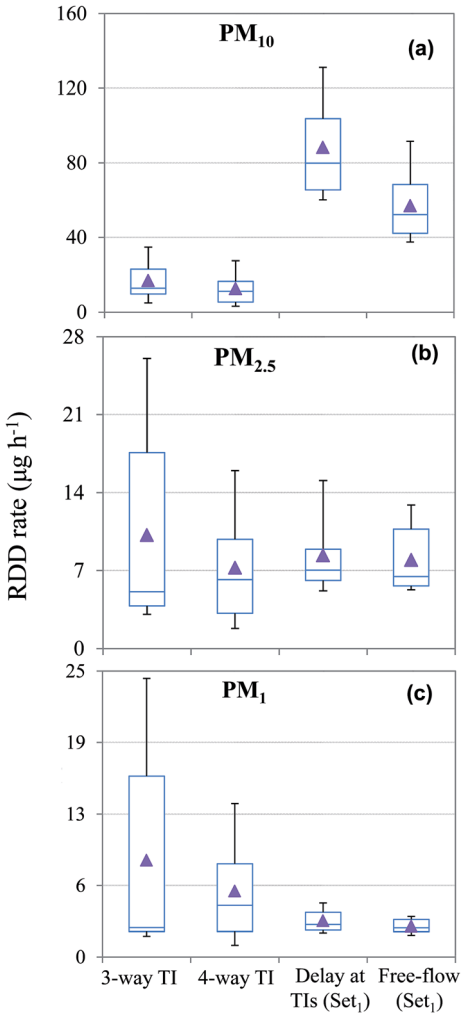

Fig. 5 Average RDD rate of (a) PM_{10}, (b) $PM_{2.5}$ and (c) PM_1 during delays at 3- and 4-way TIs and during a delay at TIs and free-flow on the rest of the route in Set_1.

Pedestrian exposure was estimated using the fixed-site measurements around the TIs (Section 3.5). Median RDD rates of PM_{10} were found to be 13 and 11 μg h^{-1} at 3- and 4-way TIs, respectively. The corresponding values for $PM_{2.5}$ were 5 and 6 μg

h^{-1} at 3- and 4-way TIs, and for PM_1 as 3 and 5 μg h^{-1} at 3- and 4-way TIs, respectively (Fig. 5a–c). These RDD rates for different PM types at 3- and 4-way TIs are close to each other. However, significant differences can be seen when the exposure data for delay and non-delay periods are segregated. For example, the on-road RDD rate of PM_{10} during delay conditions was 6.2- and 7.3-times higher than those for a pedestrian at 3- and 4-way TIs, respectively. The corresponding ratios for $PM_{2.5}$ decreased 1.4- and 1.2-times at 3- and 4-way TIs, respectively (Fig. 5a–c). These observations suggest a disproportional increase in coarse and fine particles during the delay conditions, with a much higher increase in the coarse fraction.

3.8.2 In-cabin exposure during mobile measurements. Fig. 6 shows the in-cabin RDD rates under four different ventilation settings during delay conditions (as defined in Section 2.5) at the TIs. Set_3 (*i.e.* windows closed and fan fully on) showed the lowest median in-cabin RDD rate of PM_{10} and $PM_{2.5}$ while the lowest RDD rate of PM_1 was found during Set_5 (*i.e.* windows closed, heating and fan switched off; Fig. 6a–c). This can be explained on the basis of the relationship between AER and RDD rates of different ventilation settings. For example, the average RDD rate during the delay period at TIs was found to decrease exponentially ($R^2 = 0.96$) for PM_{10} and logarithmically ($R^2 = 0.98$) for $PM_{2.5}$ with increasing AER values (ESI Fig. S7a and b†). Conversely, the average RDD rate of PM_1 was found to increase logarithmically ($R^2 = 0.62$) with increasing AER values (ESI Fig. S7c†).

The above discussion suggests that Set_3 is the best setting, resulting in 54 and 68% decrease in in-cabin PM_{10} and $PM_{2.5}$, respectively, compared with on-road RDD rate during delay conditions at TIs (Fig. 6). Likewise, Set_5 emerged as the best setting for PM_1, resulting in 76% reduction in in-cabin PM_1 during delay conditions at TIs compared with the corresponding values of on-road RDD rates (Fig. 6d). In case a most optimal setting needs to be selected to reduce in-cabin exposure to all three PM fractions, Set_5 may be considered since it results in maximum reduction in the in-cabin RDD rate of PM_1 and ~42% and 59% reduction in the in-cabin RDD rates of PM_{10} and $PM_{2.5}$, respectively. Of course, the choice of optimal setting could change to Set_3 if the highest reduction in PM_{10} or $PM_{2.5}$ is considered as a primary choice.

4. Summary, conclusion and future research

We carried out "mobile" and "fixed-site" measurements for size-resolved PMCs in the 0.25–34 μm size range in a typical UK town Guildford, Surrey. The mobile measurements were carried out on a 6 km long round route at 10 TIs. Fixed-site monitoring was carried out at two different types (*i.e.* 3- and 4-way) of TIs. The aims were to (i) assess the effects of five different ventilation settings on in-cabin PMCs on the overall route and during delay conditions at the TIs; (ii) estimate the ZoI of PM_{10}, $PM_{2.5}$ and PM_1 during stop-and-go and multiple stopping driving conditions at the TIs; (iii) estimate in-cabin exposure to PM types and compare with pedestrian exposure at TIs, and (iv) understand the range of exposure doses to which people get exposed most

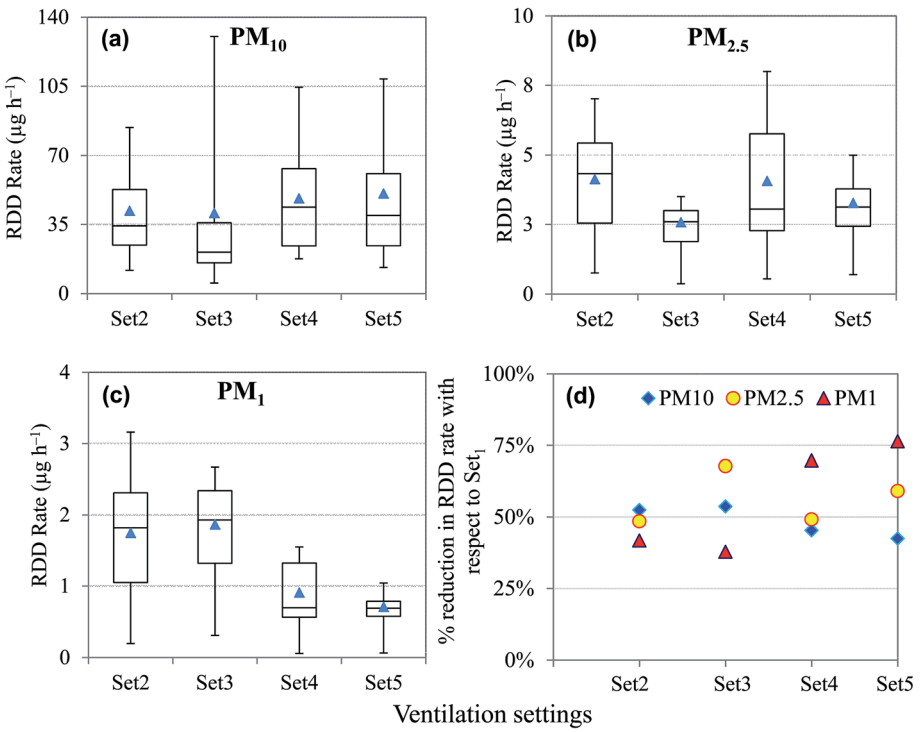

Fig. 6 Average RDD rate of (a) PM_{10}, (b) $PM_{2.5}$ and (c) PM_1 during delay conditions at TIs in Set_2, Set_3, Set_4 and Set_5. (d) Percentage reduction in in-cabin RDD rate during different ventilation settings with respect to on-road RDD rate during delay conditions at TIs. Please note that numbers on the *x*-axis represent the corresponding ventilation setting.

frequently at different types of TIs. The pdfs were fitted to fixed-site data of PM_{10}, $PM_{2.5}$ and PM_1 using a statistical distribution fitting tool (Easyfit). Based on the ranking of the fitted distributions, the "best" and most "common" pdfs were identified at both the 3- and 4-way TIs.

The following conclusions are drawn:

• The in-cabin concentration of coarse and fine particles was affected differently by the AER. Contrary to fine particles, concentrations of coarse particles ($PM_{2.5-10}$) decreased with an increase in AER.

• Median PM_{10}, $PM_{2.5}$ and PM_1 concentrations during delay periods at TIs were up to 40, 16 and 17% higher than those during free-flow conditions, indicating that TIs become hotspots of PMCs during delay conditions.

• The built-up area around the TIs did not show much impact on median PM_{10} concentration as opposed to median $PM_{2.5}$ and PM_1 that were highest at $TI_{4w\text{-}wb}$ due to the relatively high traffic volume and surrounding built-up area limiting the dispersion.

• Our results showed the existence of a ZoI within the vicinity of a TI and that the length of a ZoI depends on the type of TI, fraction of PM, and traffic driving conditions. For stop-and-go driving conditions, the ZoI was found to depend on the average acceleration and driving speed of traffic.

• Based on the fitting of the pdf to the PM data at the fixed-site, the hourly averaged PM_{10}, $PM_{2.5}$ and PM_1 concentrations over the entire fixed-site measurements at the 3-way TI were found to exceed their corresponding values during free-flow traffic conditions from mobile measurements for 41%, 34% and 35% of the total monitoring duration, respectively. The corresponding exceedances at the 4-way TI were 24%, 35% and 40%, respectively. It indicates that the frequency of exceedance increases with a decrease in the size of the particles.

• On an average, only about 7% of the commuting time spent under delay conditions at TIs over all the runs was found to contribute 10, 7 and 8% of the total commuting exposure to PM_{10}, $PM_{2.5}$ and PM_1, respectively. This indicates that TIs become hotspots of PM during delay conditions. Exposure to on-road PM_{10} under delay conditions at the TIs was 6.2- and 7.3-times higher than that for a pedestrian at 3- and 4-way TIs, respectively. The corresponding ratios for $PM_{2.5}$ were 1.4 and 1.2 at 3- and 4-way TIs, respectively.

• Set_5 (*i.e.* windows closed, fan and heating switched off) under delay conditions was found to be the optimal ventilation setting for in-cabin exposure at the TIs, leading to the highest reduction in the in-cabin RDD rate of PM_1 (76%) and significant reduction in the in-cabin RDD rate of PM_{10} (42%) and $PM_{2.5}$ (59%) with respect to the on-road RDD rate (Set_1).

This study presents hitherto missing information related to the effect of different ventilation settings and driving conditions on the PMCs and associated exposure at and around the TIs. In this study, we carried out mobile measurements on a single vehicle, further measurements to understand the effect of age, cabin space and filter types of different cars on in-cabin PMC exposure are recommended. Further fixed-site measurements around TIs with varying built-up area would also be valuable to advance the understanding of the extent of exposure around TIs.

Acknowledgements

The authors thank the UK Commonwealth Commission, Prof Alan Robins, Mr Shobhan Navaratnarajah, Mr Mihai Pop, Mr Vikas Ganesh, Mr Ganesh Chandrashekran, Mr Santosh Tirunagari, St. Saviours Church in Guildford, Departments of Estate and Facilities and the Civil & Environmental Engineering at the University of Surrey (UK), for their help during experiments and discussion. PK acknowledges the funding received from the University Global Partnership Network (UGPN) through the project "Comparison of Air Pollution in Transportation ENvironments (CAPTEN): Development and Demonstration Based on Selected UK and US Cities" for supporting this research work.

References

1 WHO, *Journal*, Ambient (Outdoor) Air Pollution Database by Country and City, United Nations, New York, 2014, http://www.who.int/phe/health_topics/outdoorair/databases/cities/en/, accessed 04.08.15.
2 R. D. Brook, S. Rajagopalan, C. A. Pope, J. R. Brook, A. Bhatnagar, A. V. Diez-Roux, F. Holguin, Y. Hong, R. V. Luepker and M. A. Mittleman, *Circulation*, 2010, **121**, 2331–2378.
3 EEA, *Air quality in the Europe–2015 report*, 2015, report ISSN 1977–8449, http://www.eea.europa.eu/publications/air-quality-in-europe-2015, EEA, accessed on 21.12.2015.
4 NHTS, Transportation, *Summary of travel trends: 2009, National household travel survey*, 2011, http://nhts.ornl.gov/2009/pub/stt.pdf, accessed on 20.10.2014.
5 A. Goel and P. Kumar, *Atmos. Environ.*, 2015, **107**, 374–390.
6 A. Goel and P. Kumar, *Atmos. Environ.*, 2015, **123**, 25–38.
7 K. H. Kim, S.-B. Lee, S. H. Woo and G.-N. Bae, *Atmos. Environ.*, 2014, **97**, 144–154.
8 USEPA, *Fed. Regist.*, 1992, **57**, 22888–22938.
9 S. Batterman, C. Jia and G. Hatzivasilis, *Environ. Res.*, 2007, **104**, 224–240.
10 M. M. Loh, J. I. Levy, J. D. Spengler, E. A. Houseman and D. H. Bennett, *Environ. Health Perspect.*, 2007, **115**, 1160–1168.
11 C. Jia, J. D'Souza and S. Batterman, *Environ. Int.*, 2008, **34**, 922–931.
12 A. Goel and P. Kumar, *Environ. Pollut.*, 2016, **214**, 54–69.
13 P. Sharma, P. Sharma, S. Jain and P. Kumar, *Atmos. Environ.*, 2013, **70**, 7–17.
14 L. Int Panis, B. de Geus, G. Vandenbulcke, H. Willems, B. Degraeuwe, N. Bleux, V. Mishra, I. Thomas and R. Meeusen, *Atmos. Environ.*, 2010, **44**, 2263–2270.
15 S. Weichenthal, K. Van Ryswyk, R. Kulka, L. Sun, L. Wallace and L. Joseph, *Environ. Sci. Technol.*, 2015, **49**, 597–605.
16 L. Suarez, S. Mesias, V. n. Iglesias, C. Silva, D. D. Caceres and P. Ruiz-Rudolph, *Environ. Sci.: Processes Impacts*, 2014, **16**, 1309–1317.
17 O. Geiss, J. Barrero-Moreno, S. Tirendi and D. Kotzias, *Aerosol Air Qual. Res.*, 2010, **10**, 581–588.
18 J. Gulliver and D. J. Briggs, *Atmos. Environ.*, 2004, **38**, 1–8.

19 L. D. Knibbs and R. J. de Dear, *Atmos. Environ.*, 2010, **44**, 3224–3227.
20 Office for National Statistics, *Census 2011: headcounts and household estimates for postcodes in England and Wales*, http://webarchive.nationalarchives.gov.uk/20160105160709/http://www.ons.gov.uk/ons/guide-method/census/2011/census-data/2011-census-data-catalogue/population-and-household-estimates/index.html, accessed on 20.07.2016.
21 Office for National Statistics, *2011 census in Surrey – car availability*, https://www.surreyi.gov.uk/ViewPage1.aspx?C=resource&ResourceID=1054&cookieCheck=true&JScript=1, accessed on 20.07.2016.
22 DoT, *Department of transport. Annual average daily traffic flows at 351 points in Surrey*, 2013, http://www.dft.gov.uk/traffic-counts/cp.php?la=Surrey, accessed on 10.07.2014.
23 F. Azarmi and P. Kumar, *Atmos. Environ.*, 2016, **137**, 62–79.
24 F. Azarmi, P. Kumar and M. Mulheron, *J. Hazard. Mater.*, 2014, **279**, 268–279.
25 F. Azarmi, P. Kumar, M. Mulheron, J. L. Colaux, C. Jeynes, S. Adhami and J. F. Watts, *J. Nanopart. Res.*, 2015, **17**, 1–19.
26 Metoffice, 2014, http://www.metoffice.gov.uk/datapoint, accessed 08.03.2015.
27 M. Mohan and T. A. Siddiqui, *Atmos. Environ.*, 1998, **32**, 3775–3781.
28 DEFRA, Department for Environment, Food & Rural Affairs, UK ambient air quality interactive maps for 2014, https://uk-air.defra.gov.uk/data/gis-mapping, accessed on 27.07.2016.
29 N. Hudda, T. Gould, K. Hartin, T. V. Larson and S. A. Fruin, *Environ. Sci. Technol.*, 2014, **48**, 6628–6635.
30 DEFRA, Air quality expert group report on fine particulate matter (PM2.5) in the United Kingdom, pp. 203, https://www.gov.uk/government/groups/air-quality-expert-group, accessed 09.06.2016.
31 C. R. Sekhar, P. Raj, P. Parida and S. Gangopadhyay, *Procedia – Social and Behavioral Sciences*, 2013, **104**, 1178–1187.
32 W. C. Hinds, *Aerosol Technology: Properties, Behaviour, and Measurement of Airborne Particles*, Wiley Interscience, 2nd edn, 1999, p. 483.
33 M. Ketzel, G. Omstedt, C. Johansson, I. Düring, M. Pohjola, D. Oettl, L. Gidhagen, P. Wåhlin, A. Lohmeyer, M. Haakana and R. Berkowicz, *Atmos. Environ.*, 2007, **41**, 9370–9385.
34 T. Kuhlbusch, A. John, H. Fissan, K.-G. Schmidt, F. Schmidt, H.-U. Pfeffer and D. Gladtke, *J. Aerosol Sci.*, 1998, **29**, S213–S214.
35 L. Y. Chan, W. L. Lau, S. C. Zou, Z. X. Cao and S. C. Lai, *Atmos. Environ.*, 2002, **36**, 5831–5840.
36 Y.-H. Cheng, *J. Occup. Environ. Hyg.*, 2008, **5**, 157–168.
37 K. C. Wang, R. E. Dickinson, L. Su and K. E. Trenberth, *Atmos. Chem. Phys.*, 2012, **12**, 9387–9398.
38 N. Hudda, E. Kostenidou, C. Sioutas, R. J. Delfino and S. A. Fruin, *Environ. Sci. Technol.*, 2011, **45**, 8691–8697.
39 P. Kumar, L. Morawska, W. Birmili, P. Paasonen, M. Hu, M. Kulmala, R. M. Harrison, L. Norford and R. Britter, *Environ. Int.*, 2014, **66**, 1–10.
40 P. Kumar, M. Ketzel, S. Vardoulakis, L. Pirjola and R. Britter, *J. Aerosol Sci.*, 2011, **42**, 580–603.
41 T. J. Barlow, P. Boulter, I. Mccrae, M. Sivell, R. Hariison, D. Carruthers and J. Stocker, *Published Project Report PPR231*, 2007.
42 Y.-W. Zhang, Z.-L. Gu, Y. Cheng, Z.-X. Shen, J.-G. Dong and S.-C. Lee, *Aerosol Air Qual. Res.*, 2012, **12**, 1261–1268.
43 A. M. Jones and R. M. Harrison, *Atmos. Environ.*, 2005, **39**, 7114–7126.
44 H.-d. He, W.-Z. Lu and Y. Xue, *Atmos. Environ.*, 2009, **43**, 6336–6342.
45 R. L. Sielken Jr and C. Valdez-Flores, *Environ. Int.*, 1999, **25**, 755–772.
46 S. Kaur, M. Nieuwenhuijsen and R. Colvile, *Atmos. Environ.*, 2005, **39**, 3629–3641.
47 M. Strak, M. Steenhof, K. J. Godri, I. Gosens, I. S. Mudway, F. R. Cassee, E. Lebret, B. Brunekreef, F. J. Kelly, R. M. Harrison, G. Hoek and N. A. H. Janssen, *Atmos. Environ.*, 2011, **45**, 4442–4453.
48 A. J. Friend, G. A. Ayoko, D. Jager, M. Wust, E. R. Jayaratne, M. Jamriska and L. Morawska, *Environ. Chem.*, 2013, **10**, 54–63.
49 P. Kumar, A. Robins, S. Vardoulakis and R. Britter, *Atmos. Environ.*, 2010, **44**, 5035–5052.
50 M. R. Heal, P. Kumar and R. M. Harrison, *Chem. Soc. Rev.*, 2012, **41**, 6606–6630.